Structural basis for m7G recognition and 2′-O-methyl discrimination in capped RNAs by the innate immune receptor RIG-I

Swapnil C. Devarkar[a,1], Chen Wang[b,1], Matthew T. Miller[b], Anand Ramanathan[a], Fuguo Jiang[b], Abdul G. Khan[b], Smita S. Patel[a,2], and Joseph Marcotrigiano[b,2]

[a]Department of Biochemistry and Molecular Biology, Robert Wood Johnson Medical School, Rutgers University, Piscataway, NJ 08854; and [b]Center for Advanced Biotechnology and Medicine, Department of Chemistry and Chemical Biology, Rutgers University, Piscataway, NJ 08854

Edited by Sun Hur, Harvard Medical School, Boston, MA, and accepted by the Editorial Board December 4, 2015 (received for review July 31, 2015)

RNAs with 5′-triphosphate (ppp) are detected in the cytoplasm principally by the innate immune receptor Retinoic Acid Inducible Gene-I (RIG-I), whose activation triggers a Type I IFN response. It is thought that self RNAs like mRNAs are not recognized by RIG-I because 5′ppp is capped by the addition of a 7-methyl guanosine (m7G) (Cap-0) and a 2′-O-methyl (2′-OMe) group to the 5′-end nucleotide ribose (Cap-1). Here we provide structural and mechanistic basis for exact roles of capping and 2′-O-methylation in evading RIG-I recognition. Surprisingly, Cap-0 and 5′ppp double-stranded (ds) RNAs bind to RIG-I with nearly identical K_d values and activate RIG-I's ATPase and cellular signaling response to similar extents. On the other hand, Cap-0 and 5′ppp single-stranded RNAs did not bind RIG-I and are signaling inactive. Three crystal structures of RIG-I complexes with dsRNAs bearing 5′OH, 5′ppp, and Cap-0 show that RIG-I can accommodate the m7G cap in a cavity created through conformational changes in the helicase-motif IVa without perturbing the ppp interactions. In contrast, Cap-1 modifications abrogate RIG-I signaling through a mechanism involving the H830 residue, which we show is crucial for discriminating between Cap-0 and Cap-1 RNAs. Furthermore, m7G capping works synergistically with 2′-O-methylation to weaken RNA affinity by 200-fold and lower ATPase activity. Interestingly, a single H830A mutation restores both high-affinity binding and signaling activity with 2′-O-methylated dsRNAs. Our work provides new structural insights into the mechanisms of host and viral immune evasion from RIG-I, explaining the complexity of cap structures over evolution.

RIG-I | capped RNA | self versus nonself | innate immunity | crystal structure

Retinoic Acid Inducible Gene-I (RIG-I) is a cytosolic innate immune receptor with the remarkable ability of distinguishing cellular self RNAs from pathogenic nonself RNAs (1, 2). RIG-I belongs to the DExH/D-box family of RNA helicases and has a multidomain architecture with three helicase domains (Hel1, Hel2, and Hel2i) located centrally, flanked by a C-terminal repressor domain (RD) and two N-terminal Caspase Activation and Recruitment Domains (CARDs) (3–7). The helicase and RD are involved in RNA recognition and binding whereas the N-terminal CARDs relay the signal to downstream factors. RIG-I is present in an inactive autoinhibited state in the absence of pathogen associated molecular pattern (PAMP) RNA ligand, but upon PAMP RNA binding, RIG-I gets activated to initiate a cell signaling response ultimately leading to Type I IFN production.

RNAs carrying a 5′-triphosphate (5′ppp) moiety and blunt-ended double-stranded (ds)RNAs are the best characterized PAMP ligands of RIG-I, showing high-affinity binding and robust stimulation of the ATP hydrolysis activity (8–10). Although RIG-I is surrounded by cellular RNAs, they do not activate RIG-I due to posttranscriptional modification of the RNA 5′ ends. The 5′ end of many cellular RNAs like mRNAs is modified with the addition of a 7-methyl guanosine (m7G) connected by a 5′-to-5′ triphosphate bridge to the first nucleotide (Cap-0) (11). In humans and other higher eukaryotes, the 5′ end is further modified with 2′-O-methylation of the first and second nucleotides ribose (Cap-1 and Cap-2, respectively) (12, 13). Viral genomic RNA or replication intermediates are specifically recognized by RIG-I due to the presence of 5′ppp. However, many viruses (e.g., influenza virus, Ebola virus, measles virus) cap their genomes and/or transcripts, which in part serves as an immune evasion mechanism (14, 15). It is believed that 5′-capping protects RNAs from RIG-I recognition; however, a clear understanding of the biochemical and structural basis of RIG-I evasion by these RNA modifications is lacking.

We use multiple approaches including X-ray crystallography, enzymology, and cell-based signaling assays to study the effects of 5′ cap and 2′-O-methylation modifications in modulating dsRNA recognition by RIG-I. Our studies assign specific roles to these modifications showing that Cap-0 dsRNAs are RIG-I PAMPs, with similar biochemical characteristics and signaling response as the 5′ppp dsRNAs, whereas Cap-1 modifications abrogate RIG-I activation. Structural studies provide new mechanistic insights into capped RNA recognition by RIG-I and the roles of m7G cap and 2′-O-methylation in immune evasion. Our findings reveal a previously unidentified family of RNAs that

Significance

The cytosolic innate immune receptor Retinoic Acid Inducible Gene-I (RIG-I) is the principal detector of pathogenic RNAs carrying a 5′-triphosphate (5′ppp). Self RNAs like mRNAs evade recognition by RIG-I due to posttranscriptional modifications like 5′-end capping with 7-methyl guanosine (m7G) and 2′-O-methylation of 5′-end nucleotides. Viruses have also evolved mechanisms to mimic these modifications, which in part is believed to aid in immune evasion. Currently, it is unclear how these modifications modulate RIG-I recognition. This paper provides structural and mechanistic insights into the roles of the m7G cap and 2′-O-methylation in RIG-I evasion. We show that RIG-I accommodates the m7G base while maintaining the 5′ppp contacts and can recognize Cap-0 RNAs but not Cap-1.

Author contributions: S.S.P. and J.M. designed research; S.C.D., C.W., A.R., F.J., and A.G.K. performed research; S.C.D., C.W., M.T.M., A.R., F.J., S.S.P., and J.M. analyzed data; and S.C.D., C.W., S.S.P., and J.M. wrote the paper.

The authors declare no conflict of interest.

This article is a PNAS Direct Submission. S.H. is a guest editor invited by the Editorial Board.

Freely available online through the PNAS open access option.

Data deposition: Crystallography, atomic coordinates, and structure factors have been deposited in the Protein Data Bank, www.pdb.org [PDB ID codes 5F98 (Helicase-RD–Cap-0 RNA structure), 5F9F (Helicase-RD–5′OH RNA structure), and 5F9H (Helicase-RD–5′ppp RNA structure)].

[1]S.C.D. and C.W. contributed equally to this work.

[2]To whom correspondence may be addressed. Email: patelss@rutgers.edu or jmarco@cabm.rutgers.edu.

This article contains supporting information online at www.pnas.org/lookup/suppl/doi:10.1073/pnas.1515152113/-/DCSupplemental.

are recognized by RIG-I and provide valuable insights into the viral immune evasive mechanisms.

Results and Discussion

RIG-I Recognizes Cap-0 dsRNAs as Efficiently as 5′ppp dsRNAs. To investigate the contribution of various 5′-end RNA modifications on RIG-I recognition of dsRNAs, chemically synthesized 10-bp blunt-ended hairpin RNAs (HP RNA) with 5′OH, 5′ppp, or 5′cap (m7G) moiety (*SI Appendix*, Table S1) were analyzed for binding affinity and ATPase turnover rates. The RNA binding affinity under ATP cycling conditions was measured by titrating RIG-I with increasing concentration of the RNA ligand (Fig. 1*A* and *SI Appendix*, Fig. S1). The data were fit to the 1:1 binding model to obtain the RNA dissociation constant ($K_{d,app}$) and the maximal ATPase turnover rate (k_{atpase}). The 5′OH HP RNA binds to RIG-I with a $K_{d,app}$ of ∼40 nM and the 5′ppp HP RNA binds to RIG-I with a 20-fold higher affinity ($K_{d,app}$ ∼2 nM) (Fig. 1*A* and Table 1). Surprisingly, the Cap-0 HP RNA binds to RIG-I with the same high affinity as the 5′ppp HP RNA ($K_{d,app}$ ∼2 nM). Furthermore, all three HP RNAs show robust stimulation of RIG-I's ATPase activity (Table 1). These results indicate that the presence of m7G cap on the 5′ppp moiety does not compromise the binding affinity or the ATPase activity of RIG-I.

We also tested the affinity and ATPase activity of RIG-I for 27 nucleotide single-stranded (ss) RNAs carrying 5′ppp or Cap-0 moiety. RIG-I showed no binding or ATPase activity with these RNAs. On the other hand, Helicase-RD RIG-I (lacking the N-terminal CARDs) showed high affinity for 5′ppp and Cap-0 ssRNAs in the range of 15–35 nM (Table 1 and *SI Appendix*, Fig. S2). Interestingly, the ssRNAs did not stimulate the Helicase-RD's ATPase activity, which was 50- to 100-fold lower than their double-stranded counterparts, suggesting that these RNAs form nonproductive complexes.

Crystal Structures of Helicase-RD RIG-I with 5′OH, 5′ppp, and Cap-0 HP RNAs. Three structures of RIG-I Helicase-RD in complex with HP RNA, identical in sequence and bearing 5′OH, ppp, or Cap-0, respectively, were determined by X-ray crystallography (Fig. 1*B* and *SI Appendix*, Table S2). All three crystals belong to space group $P2_12_12_1$ with six complexes of Helicase-RD–RNA per asymmetric unit, yielding six independent views of the complex. The total 18 copies of the Helicase-RD protein, from the three structures, are nearly identical, with a root mean square deviation (rmsd) of less than 0.7 Å for similar carbon alpha atoms. This analysis indicates that the presence of 5′ppp and Cap-0 does not perturb the overall structure of the Helicase-RD.

Interestingly, comparing the helicase domain from our Helicase-RD–5′ppp HP RNA complex with the previously reported structures of Helicase-RD bound to 5′ppp 8-bp HP RNA [Protein Data Bank (PDB) ID 4AY2] (16) and the unliganded duck RIG-I (PDB ID 4A2W) (5) yielded rmsds of 3.8 Å and 6.2 Å, respectively for similar backbone atoms (*SI Appendix*, Fig. S3*A*). Although both 4AY2 and our structure with 5′ppp HP RNA used human RIG-I, the helicase domain in 4AY2 has fewer interactions with the RNA and is more closely similar to the unliganded RIG-I (4A2W) (rmsd of 2.8 Å for the helicase domains of 4AY2 and 4A2W). Therefore, the discrepancy between the current 5′ppp structure and 4AY2 is likely due to the presence of a disulfide bond in the Hel2i of 4AY2, different crystallization conditions, or different crystal packing arrangement (16, 17).

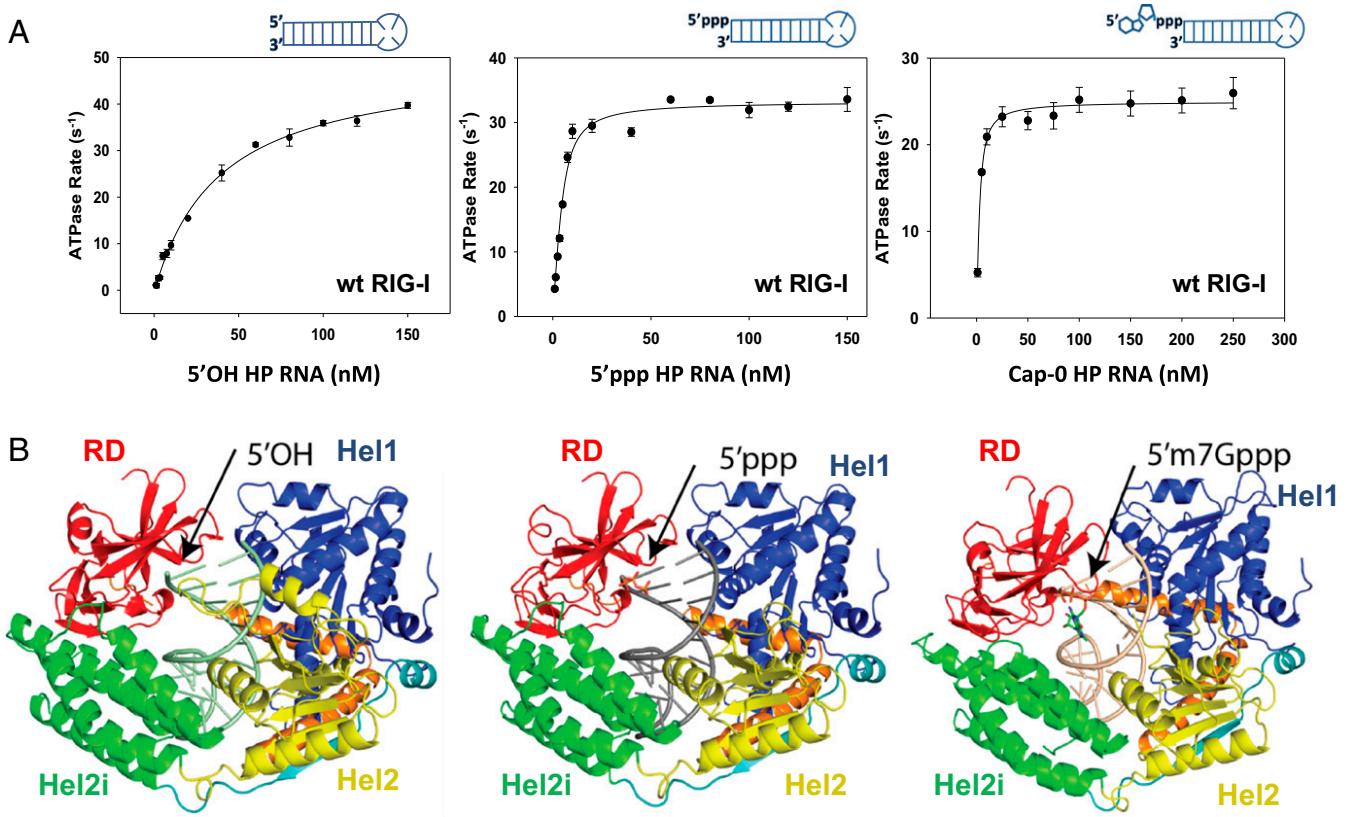

Fig. 1. K_d, ATP hydrolysis rate, and crystal structures of the RIG-I complexes with hairpin RNA containing 5′OH, 5′ppp, and Cap-0 end-modifications. (*A*) The ATP hydrolysis rate of RIG-I measured at 37 °C in Buffer A is plotted against increasing concentrations of 5′OH, 5′ppp, and m7G cap HP RNA. Schematic representations of the RNAs are shown. The dependencies were fit to Eq. **2** to obtain the $K_{d,app}$ and k_{atpase} (Table 1). (*B*) Overview of the crystal structure of Helicase-RD in complex with 5′OH HP RNA (PDB ID 5F9F) (*Left*), 5′ppp HP RNA (PDB ID 5F9H) (*Center*), and Cap-0 HP RNA (PDB ID 5F98) (*Right*).

Table 1. RNA binding and ATPase activity of WT RIG-I and Helicase-RD

	WT RIG-I		Helicase-RD	
RNA ligand	$K_{d,app}$, nM	k_{atpase}, s^{-1}	$K_{d,app}$, nM	k_{atpase}, s^{-1}
5′OH HP RNA	38.5 ± 4	49 ± 1	0.4 ± 0.3	63 ± 1
5′ppp HP RNA	1.8 ± 0.9	33 ± 0.9	0.75 ± 0.3	48 ± 1
Cap-0 HP RNA	1.7 ± 0.5	25 ± 0.4	0.08 ± 0.04	36 ± 0.4
5′ppp ssRNA	N.B.	N.B.	35 ± 5.5	0.9 ± 0.03
Cap-0 ssRNA	N.B.	N.B.	14 ± 4.4	0.3 ± 0.03

N.B., no binding detected.

Conformational Changes in Helicase Motif IVa Accommodates 5′ppp and Cap-0 dsRNA. A major difference between the structures of Helicase-RD bound to 5′OH HP RNA compared with 5′ppp and Cap-0 RNAs lies in the helicase motif IVa, which is located in the Hel2 region of RIG-I (residues 664–685) and highly conserved in the SF2 family of helicases (18). The helicase motif IVa is disordered in the absence of RNA (4A2W) and in the presence of 5′ppp or Cap-0 RNAs. However, this motif adopts an extended loop structure followed by a short alpha helix in the presence of 5′OH RNA (Fig. 2*A*). The loop (664–673) in the 5′OH HP RNA complex structure is in close proximity to the blunt end of the HP RNA. The short alpha helix (673–685) in the motif IVa of RIG-I sits approximately perpendicular to the RNA axis. Superposition of the three structures shows that the Hel2 loop clashes with the 5′ppp and the m7G moieties (*SI Appendix*, Fig. S3*B*). Thus, disruption of motif IVa structure results in a cavity between the RD and Hel2i that accommodates the 5′ppp and the m7G moiety (*SI Appendix*, Fig. S3*C*). Although disordered in the 5′ppp and Cap-0 structures, motif IVa is important for RIG-I function, because its deletion inactivates RIG-I signaling (*SI Appendix*, Fig. S4). Interestingly, the corresponding loop in the MDA5 interacts with the major groove of the dsRNA, and deleting this loop leads to defects in MDA5′s ATPase and signaling function (19).

RIG-I Accommodates the m7G Cap Without Perturbation of the ppp Moiety Interactions. The HP RNAs in all complexes are in a nearly identical conformation with an rmsd of 0.6 Å for similar backbone atoms (Fig. 2*B*). Interpretable density for the 5′ppp moiety is clearly discernable in all copies of the 5′ppp and Cap-0 dsRNA and superimpose well (Fig. 2*C*). However, the spatial distribution of the ribose and m7G positions varies in the Cap-0 dsRNAs (*SI Appendix*, Fig. S5). Although there is interpretable density for each Cap-0 ribose, only three out of the six complexes in the asymmetric unit have density for the m7G base. This variability could be due to crystal packing interactions that stabilize regions around the cap-binding cavity. Furthermore, each m7G in the

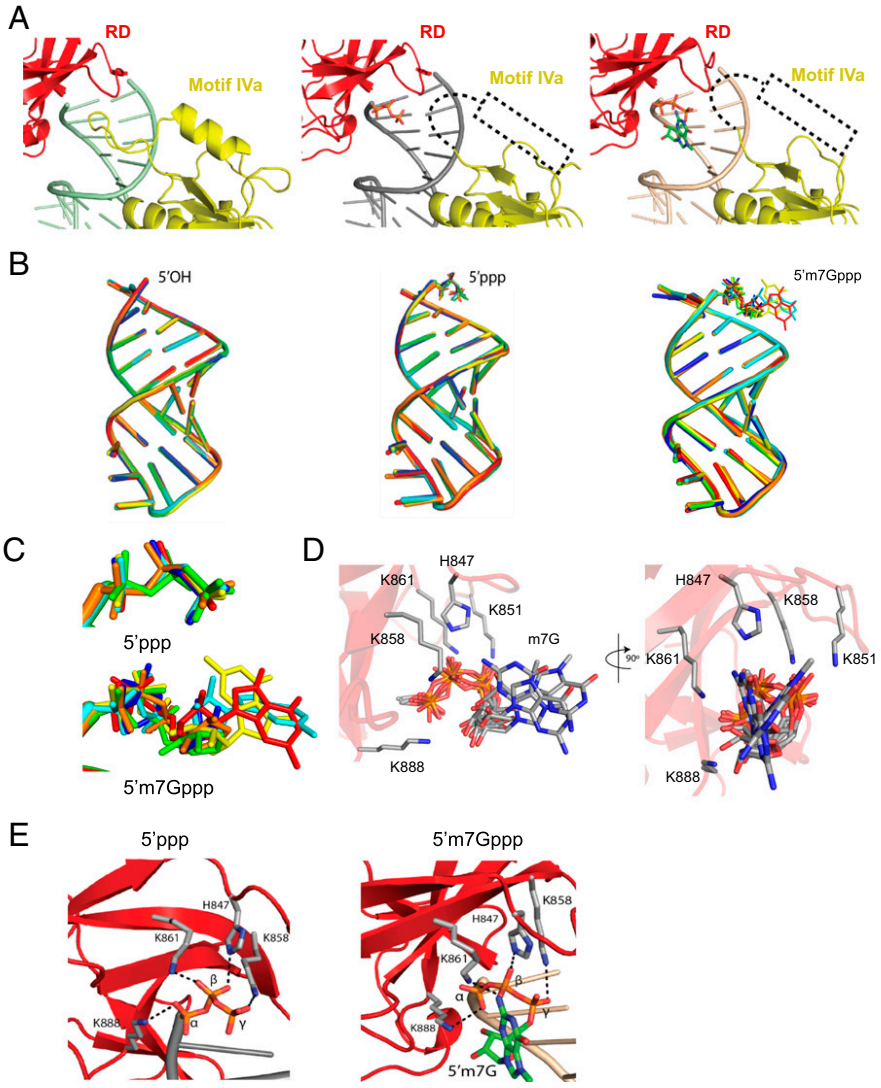

Fig. 2. Interactions of RIG-I with the 5′ppp and Cap-0 end-modifications. (*A*) Magnified view of Hel2 and RD interaction with 5′OH HP RNA (*Left*), 5′ppp HP RNA (*Center*), and Cap-0 HP RNA (*Right*). The Hel2 loop-helix region (664–685) in the helicase motif IVa is ordered in the presence of 5′OH and disordered (dashed line) in the presence of 5′ppp and Cap-0. (*B*) The RNA ligands from the six complexes in the asymmetric unit for each crystal are superimposed using the protein for the calculation. Each color represents one of the six complexes in each unit cell. (*C*) Magnified view of the overlaid 5′ppp and m7Gppp moiety from *B*. (*D*) Superimposition of the m7Gppp moiety from the six complexes of the asymmetric unit is shown. Highlighted are conserved contacts within 4 Å of the m7Gppp moiety. The view in *Right* is rotated 90° about a vertical axis. No conserved specific contacts with the m7G were observed. (*E*) Magnified view of the protein contacts of the 5′ppp moiety in the 5′ppp HP and Cap-0 HP RNA structures.

three complexes has a slightly different conformation, suggesting that the base is highly mobile. Besides, there are no conserved interactions with the m7G moiety in the six complexes (Fig. 2*D* and *SI Appendix*, Fig. S6). This data indicates that RIG-I accommodates m7G without cap specific interactions seen in many cap binding proteins like the translation initiation factor, eIF4E (20, 21). Overall, the structural data are consistent with the biochemical data showing nearly identical binding affinities of RIG-I for 5′ppp and Cap-0 HP RNA (Fig. 1*A* and Table 1).

The 5′ppp is coordinated by a group of conserved basic residues (K858, K861, K888, and H847) in both the 5′ppp and Cap-0 structures (Fig. 2*E*) as seen in previously reported structures (6, 7, 16). However, in contrast to structures of RD with 5′pp 12-bp dsRNA (PDB ID 3NCU) and Helicase-RD with 8-bp 5′ppp HP RNA (PDB ID 4AY2), the gamma phosphate is in close proximity to K858 in both 5′ppp and Cap-0 HP RNA structures. This interaction was reported in the structure of RD with 5′ppp 14bp dsRNA (PDB ID 3LRN) (6, 7, 16).

H830 Residue Is the Primary Sensor of 2′-O-Methylation in Cap-1 dsRNA. The 2′OH of the first nucleotide ribose at the 5′-end of RNA is in close proximity to histidine 830 (H830) (Fig. 3 *A* and *B*) (3–6, 16). In higher eukaryotes, the m7G capping reaction is accompanied by 2′-O-methylation of the first and second nucleotide ribose resulting in Cap-1 and Cap-2 RNAs, respectively (12, 13). Based on the structures, we predicted that 2′-O-methylation of the first ribose will clash with the H830 residue of RIG-I. We therefore set out to analyze the effects of 2′-O-methylation of the first nucleotide ribose of the 5′ppp and Cap-0 HP RNAs on the binding affinity and ATPase activity of RIG-I (Fig. 3 *C* and *D* and Table 2). The 2′-O-methylated 5′ppp HP RNA has a 20-fold lower binding affinity ($K_{d,app}$ = 40 nM) and twofold lower ATPase turnover rate (k_{atpase} = 12 s^{-1}) compared with unmethylated RNA. Curiously, this is not a large effect on the binding affinity. Interestingly, 2′-O-methylated Cap-0 HP RNA showed a drastic 200-fold decrease in binding affinity ($K_{d,app}$ = 425 nM) and twofold lower ATPase turnover rate (k_{atpase} = 15 s^{-1}). These results indicate that 2′-O-methylation works synergistically with m7G cap to lower RNA binding affinity.

In contrast to WT RIG-I, H830A binds 2′-O-methylated 5′ppp HP RNA and Cap-1 HP RNA with almost the same affinity as the unmethylated dsRNAs (Table 2) and shows wild-type like ATPase turnover rates (Fig. 3 *E* and *F*). Thus, H830A mutation rescues the deleterious effects of 2′-O-methylation. The structure also shows that V886 is in close proximity (~4 Å) to the 2′OH group of the first 5′-end nucleotide ribose (Fig. 3 *A* and *B*). However, V886A in conjunction with H830A mutation did not enhance the rescue effect (*SI Appendix*, Fig. S7*A*). Thus,

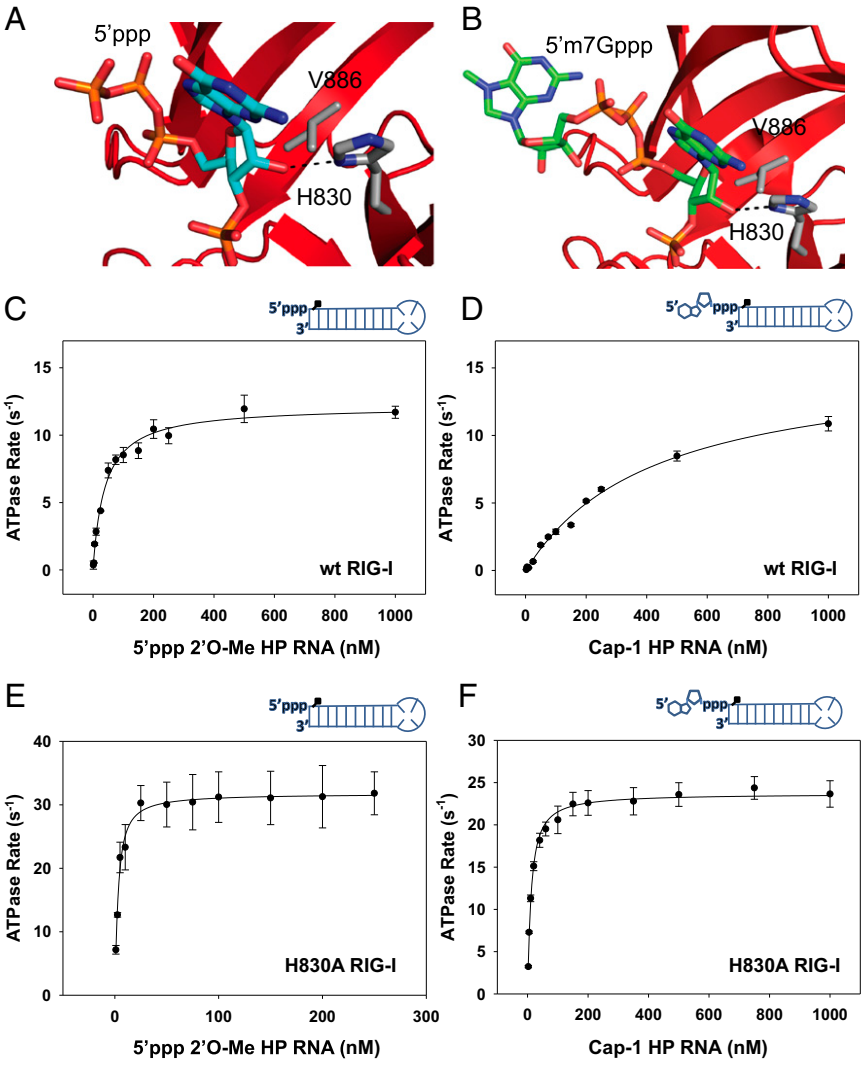

Fig. 3. K_d and ATP hydrolysis rate of RNA complexes with WT and H830A RIG-I. (*A* and *B*) A magnified view of RIG-I contacts with the 2′ hydroxyl groups of the first nucleotide ribose in the crystal structure of Helicase-RD with 5′ppp HP RNA (*A*) and Cap-0 HP RNA (*B*). (*C* and *D*) The ATP hydrolysis rate of WT RIG-I is plotted against increasing concentrations of 5′ppp 2′-OMe HP RNA (*C*) and Cap-1 HP RNA (*D*). (*E* and *F*) The ATP hydrolysis rate of H830A RIG-I is plotted against increasing concentrations of 5′ppp 2′-OMe HP RNA (*E*) and Cap-1 HP RNA (*F*). The dependencies were fit to Eq. **2** to obtain the $K_{d,app}$ and k_{atpase} values (Table 2).

Table 2. RNA binding and ATPase activity of WT RIG-I and H830A RIG-I

RNA ligand	WT RIG-I		H830A RIG-I	
	$K_{d,app}$, nM	k_{atpase}, s^{-1}	$K_{d,app}$, nM	k_{atpase}, s^{-1}
5′ppp HP RNA	1.8 ± 0.9	33 ± 0.9	1.6 ± 1.9	34 ± 1
5′ppp 2′-OMe HP RNA	40 ± 6	12 ± 0.4	2.3 ± 0.7	32 ± 0.5
Cap-0 HP RNA	1.7 ± 0.5	25 ± 0.4	1.9 ± 0.5	22 ± 0.4
Cap-1 HP RNA	425 ± 50	15 ± 0.7	9.5 ± 2	24 ± 0.3

H830 is the primary sensor for 2′-O-methylation of the first nucleotide ribose in Cap-1 RNAs.

Signaling Response of RIG-I and H830A RIG-I to Capped dsRNAs. To put these biochemical and structural results into cellular context, the various 5′-end modified dsRNA were tested in cell-based signaling assays using HEK293T cells. We used 27-bp dsRNAs with various 5′-end modifications on one end and a three-nucleotide 5′ overhang (5′ovg) on the other end (Fig. 4*A*). Longer RNAs have a more robust cell signaling response (8). Mock-transfected cells (empty plasmid) did not show any detectable signal when stimulated with RNAs (*SI Appendix*, Fig. S7*B*). However, ectopic expression of RIG-I results in a background signal in the absence of transfected RNAs that was negated from the signal produced (22). When the cells expressing WT RIG-I were stimulated with increasing concentration of 5′ppp dsRNA, a signaling response was observed with as low as 5 nM RNA (Fig. 4*B*, blue bars), and a similar signaling response was observed with the Cap-0 dsRNA (Fig. 4*B*, red bars). The concentration dependencies of the 5′ppp dsRNA and Cap-0 dsRNA follow an almost identical trend. These results clearly demonstrate that RIG-I is activated by Cap-0 dsRNAs.

In contrast, Cap-1 dsRNA exhibits substantially lower signaling activity even at high RNA concentrations (~700 nM) (Fig. 4*C*, blue bars), consistent with its weak binding affinity and low ATPase activity. The low signal from Cap-1 dsRNA is most probably a background signal due to the 5′ovg on the opposite end, as dsRNA with 5′ overhangs on both ends also showed an identical low signaling response (Fig. 4*C*). We also found that the signaling response of the 5′ppp HP RNA was abolished when the ribose of the first nucleotide was 2′-O-methylated (*SI Appendix*, Fig. S7*C*), consistent with previous reports (23) even though this modified RNA binds to RIG-I with a comparatively high affinity ($K_{d,app}$ ~40 nM). Overall, these results demonstrate that 2′-O-methylation and not Cap-0 is the critical modification responsible for RIG-I evasion.

Cells expressing H830A RIG-I are activated by 5′ppp and Cap-0 RNAs, with a similar concentration dependency as WT RIG-I (Fig. 4*B*). However, unlike WT RIG-I, cells expressing H830A RIG-I elicited a signaling response for Cap-1 dsRNA and 5′ppp 2′O-Me HP RNA (Fig. 4*C*, red bars and *SI Appendix*, Fig. S7*C*). Interestingly, Cap-0 dsRNA activates H830A better than WT RIG-I. Similarly, H830A RIG-I shows a twofold higher background signal in the absence of RNA stimulation, compared with WT RIG-I (*SI Appendix*, Fig. S7*B*). Because the expression levels of H830A and WT RIG-I are comparable (Fig. 4*D*), this observation suggests that H830A RIG-I is activated by cellular RNAs. A recent study (23) similarly showed that cellular RNAs activate H830A and that the activity of Cap-1 methyltansferase enzyme, MTr1, suppresses WT RIG-I activation by endogenous RNAs, but showed no such effect on H830A. Taken together, the biochemical, structural, and cell-based studies indicate that the H830 residue is crucial for discriminating between Cap-0 and Cap-1 RNAs.

RIG-I Is Not Activated by Short 5′ppp and Cap-0 ssRNA. We also tested chemically synthesized 27-mer 5′ppp and Cap-0 ssRNAs for RIG-I activation. In contrast to dsRNAs, the 5′ppp and Cap-0 ssRNAs did not elicit a signaling response (Fig. 4*E* and *SI Appendix*, Fig. S8). These results are consistent with our biochemical studies showing no detectable binding or ATPase activity of RIG-I with these ssRNAs (Table 1 and *SI Appendix*, Fig. S2). The results imply that capped mRNA ends in cells that are single-stranded will not activate RIG-I.

Complementary Roles of IFIT1 and RIG-I in Cap-0 RNA Recognition. IFIT1 is an IFN stimulated receptor recently shown as a key player in the recognition of capped RNAs (24). IFIT1 recognizes ssRNAs with 5′ppp and implicated in the recognition of Cap-0 RNAs but not Cap-1 RNAs (25). RIG-I recognizes base paired RNAs with 5′ppp or Cap-0, but not short ssRNAs. This observation is consistent with structural studies of RIG-I and IFIT1 that

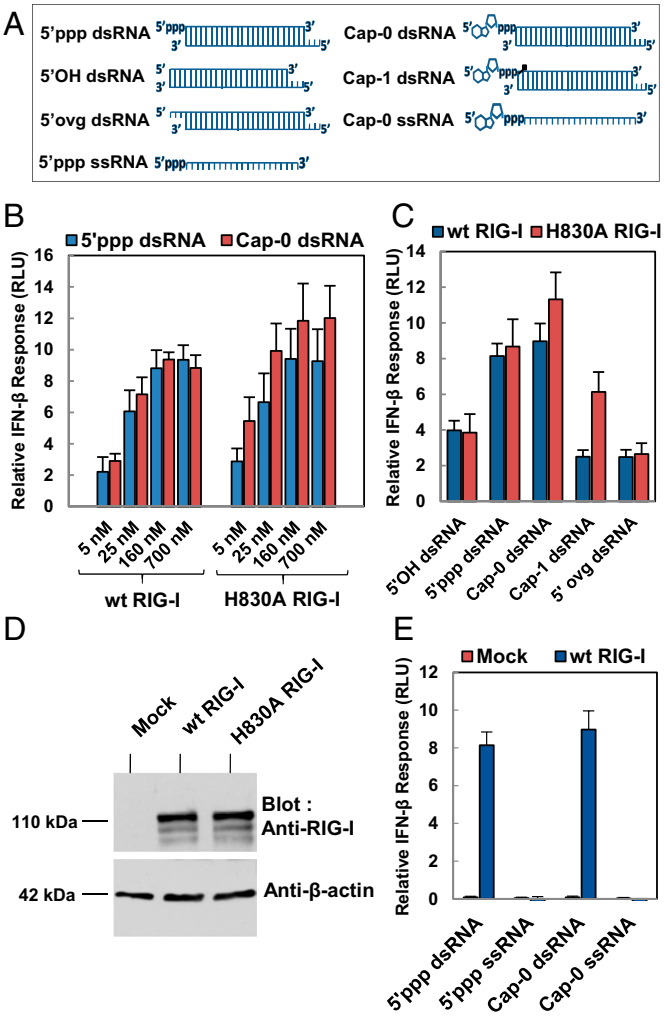

Fig. 4. Cell-based signaling assays to measure RIG-I activation by RNAs with various 5′-end modifications. (*A*) Schematic representation of all of the RNA ligands used in the cell-based signaling studies (27-bp dsRNAs and 27-mer ssRNAs). (*B*) The luciferase signal is plotted as the IFN-β response of WT RIG-I or H830A RIG-I transfected cells stimulated with various concentration of 5′ppp dsRNA (blue bars) and Cap-0 dsRNA (red bars). (*C*) The luciferase signal is plotted as the IFN-β response of WT RIG-I (blue bars) or H830A RIG-I (red bars) stimulated with the indicated RNA ligand. (*D*) Western blot analysis of cell lysates from mock, WT RIG-I, and H830A RIG-I–transfected cells, probed with anti–RIG-I and anti–β-actin antibodies. (*E*) The luciferase signal is plotted as the IFN-β response of mock or WT RIG-I stimulated with the indicated RNA ligand. Signaling data were collected from quadruplicate sets, and the SEM is shown as error bars.

show that these molecules are tailored for binding base paired RNAs and ssRNAs, respectively (3–6, 26, 27). Thus, it appears that the roles of RIG-I and IFIT1 are complementary to each other.

The 2′-O-methylation of 5′-end nucleotide is the essential modification to avoid recognition by RIG-I and residue H830 is the sensor for this modification on Cap-1 RNAs. RIG-I is found only in higher eukaryotes like humans and other vertebrates, and this coincides with the emergence of 2′-O-methyltransferases over the course of evolution (28). All human cellular mRNAs bear either Cap-1 or Cap-2 structures, and based on our findings such RNAs cannot activate RIG-I, regardless of single-stranded or double-stranded ends. A common feature of some of the most pernicious viruses like Ebola and Marburg virus is the evolution of capping mechanisms and 2′-O-methyltransferase activities, facilitating the viral RNA transcripts to closely mimic cellular Cap-1 RNAs. The viral titers of Yellow fever virus were drastically reduced in A549 and Vero cell lines when its 2′-O-methyltransferase activity was abrogated, and this effect was shown to be mediated by RIG-I (23). Thus, viral 2′-O-methyltransferase enzymes are prime targets for designing effective antiviral therapies.

In summary, before this and another study (23), it was hypothesized that discrimination of self from nonself RNA was due to the presence of the m7G moiety, which was thought to sterically hinder binding to RIG-I. This presumption is not true because dsRNAs with m7G show comparable binding affinity, ATPase, and cell signaling activity as dsRNAs with a 5′ triphosphate. Our structural studies provide the exact mechanism for binding of capped RNAs by RIG-I by providing insights into the nature of interactions between RIG-I and the 5′m7Gppp moiety. Interestingly, RIG-I makes no specific interactions with the m7G, but instead accommodates its presence through the disordering of helicase motif IVa. The interactions of RIG-I with the ppp of the Cap-0 RNA were identical to that seen in the case of 5′ppp HP RNA, as evident in their respective structures.

These new insights can be used in the design of ligands or therapeutics to either stimulate or inhibit RIG-I activity, depending on the desired outcome. For example, the triphosphorylated dsRNA has high binding affinity and signaling activity; however, the triphosphate moiety can be easily degraded by cellular phosphatases. In cells, the m7G cap serves to increase the half-life of the RNA by circumventing 5′-end degradation. However, the cap has additional roles in translation initiation, nuclear export, etc. The structure of RIG-I in complex with Cap-0 RNA will be useful for modeling of naturally-occurring and designer chemical moieties on the 5′ppp that will increase the half-life of the RNA while preventing interactions with other cap-binding proteins (e.g., the translation initiation factor eIF4E). The moiety may itself serve a specific function, such as to act as an activator or inhibitor of another cellular protein, or target the RNA ligand to specific cell types. Similar to the m7G, RIG-I can accommodate 2-nucleotide 3′-overhangs such as those in siRNAs (29). The 5′ppp containing siRNAs have been used to knock down expression of specific oncogenes in cancer cells as well as stimulate RIG-I to induce apoptosis in the cancer cell (30). Conversely, it may be advantageous to design an RNA for a specific cellular function without stimulating RIG-I activity by modifying the 2′ position of the first base.

Materials and Methods

All of the RNAs used in the study were chemically synthesized, HPLC purified, and analyzed by mass spectrometry (*SI Appendix*, Table S1 and Fig. S8). The proteins were expressed and purified from recombinant Rosetta DE3 *Escherichia coli* cell line, as described (3). The RNA K_d values and the ATPase turnover rates were measured using [γ^{32}P] ATP and PEI-cellulose TLC. The complexes of Helicase-RD with the RNA ligands were purified by gel filtration and cocrystallized. Crystals of Helicase-RD–Cap-0 HP RNA complex were grown in 20% (wt/vol) PEG 3350, 0.2 M NaSCN, 0.1 M MOPS (pH 7.8), 3.5% (vol/vol) 2,2,2-trifluoroethanol. Crystals of Helicase-RD–5′ppp HP RNA complex were grown from 23% (wt/vol) PEG 3350, 0.25 M KSCN, 0.1 M MOPS (pH 7.8). Crystals of Helicase-RD–5′OH HP RNA complex were obtained in similar conditions as Helicase-RD–5′ppp HP RNA complex, except 0.3 M NaSCN was used instead of 0.25 M KSCN. Signaling assays were carried out in HEK293T cell line by using the Promega Dual Luciferase Assay kit. Detailed protocols for RNA preparation, ATPase assay, complex formation and crystallization, signaling assay, and Western blot are described in *SI Appendix*, *SI Materials and Methods*.

ACKNOWLEDGMENTS. We acknowledge access to beamlines X25 at the National Synchrotron Light Source (NSLS), 8.3.1 at Advanced Light Source (ALS), and F1 at Cornell High Energy Synchrotron Source (CHESS) and thank the NSLS, ALS, and CHESS staff. We thank T. Fujita and M. Gale Jr., for providing the mammalian expression constructs; and E. Arnold, S. K. Burley, P. Lobel, T. Saleh, A. Shatkin, and members of the S.S.P. and J.M. laboratories for providing helpful comments and assistance. This work was supported by NIH Grant GM111959 (to J.M. and S.S.P.).

1. Yoneyama M, et al. (2005) Shared and unique functions of the DExD/H-box helicases RIG-I, MDA5, and LGP2 in antiviral innate immunity. *J Immunol* 175(5):2851–2858.
2. Yoneyama M, et al. (2004) The RNA helicase RIG-I has an essential function in double-stranded RNA-induced innate antiviral responses. *Nat Immunol* 5(7):730–737.
3. Jiang F, et al. (2011) Structural basis of RNA recognition and activation by innate immune receptor RIG-I. *Nature* 479(7373):423–427.
4. Luo D, et al. (2011) Structural insights into RNA recognition by RIG-I. *Cell* 147(2):409–422.
5. Kowalinski E, et al. (2011) Structural basis for the activation of innate immune pattern-recognition receptor RIG-I by viral RNA. *Cell* 147(2):423–435.
6. Wang Y, et al. (2010) Structural and functional insights into 5′-ppp RNA pattern recognition by the innate immune receptor RIG-I. *Nat Struct Mol Biol* 17(7):781–787.
7. Lu C, et al. (2010) The structural basis of 5′ triphosphate double-stranded RNA recognition by RIG-I C-terminal domain. *Structure* 18(8):1032–1043.
8. Schlee M, et al. (2009) Recognition of 5′ triphosphate by RIG-I helicase requires short blunt double-stranded RNA as contained in panhandle of negative-strand virus. *Immunity* 31(1):25–34.
9. Hornung V, et al. (2006) 5′-Triphosphate RNA is the ligand for RIG-I. *Science* 314(5801): 994–997.
10. Kohlway A, Luo D, Rawling DC, Ding SC, Pyle AM (2013) Defining the functional determinants for RNA surveillance by RIG-I. *EMBO Rep* 14(9):772–779.
11. Shatkin AJ (1976) Capping of eucaryotic mRNAs. *Cell* 9(4 PT 2):645–653.
12. Filipowicz W, et al. (1976) A protein binding the methylated 5′-terminal sequence, m7GpppN, of eukaryotic messenger RNA. *Proc Natl Acad Sci USA* 73(5):1559–1563.
13. Furuichi Y, Shatkin AJ (2000) Viral and cellular mRNA capping: Past and prospects. *Adv Virus Res* 55:135–184.
14. Hyde JL, Diamond MS (2015) Innate immune restriction and antagonism of viral RNA lacking 2′-O methylation. *Virology* 479-480:66–74.
15. Decroly E, Ferron F, Lescar J, Canard B (2012) Conventional and unconventional mechanisms for capping viral mRNA. *Nat Rev Microbiol* 10(1):51–65.
16. Luo D, Kohlway A, Vela A, Pyle AM (2012) Visualizing the determinants of viral RNA recognition by innate immune sensor RIG-I. *Structure* 20(11):1983–1988.
17. Kolakofsky D, Kowalinski E, Cusack S (2012) A structure-based model of RIG-I activation. *RNA* 18(12):2118–2127.
18. Fairman-Williams ME, Guenther UP, Jankowsky E (2010) SF1 and SF2 helicases: Family matters. *Curr Opin Struct Biol* 20(3):313–324.
19. Wu B, et al. (2013) Structural basis for dsRNA recognition, filament formation, and antiviral signal activation by MDA5. *Cell* 152(1-2):276–289.
20. Marcotrigiano J, Gingras AC, Sonenberg N, Burley SK (1997) Cocrystal structure of the messenger RNA 5′ cap-binding protein (eIF4E) bound to 7-methyl-GDP. *Cell* 89(6):951–961.
21. Topisirovic I, Svitkin YV, Sonenberg N, Shatkin AJ (2011) Cap and cap-binding proteins in the control of gene expression. *Wiley Interdiscip Rev RNA* 2(2):277–298.
22. Bamming D, Horvath CM (2009) Regulation of signal transduction by enzymatically inactive antiviral RNA helicase proteins MDA5, RIG-I, and LGP2. *J Biol Chem* 284(15): 9700–9712.
23. Schuberth-Wagner C, et al. (2015) A conserved histidine in the RNA sensor RIG-I controls immune tolerance to N-2′O-methylated self RNA. *Immunity* 43(1):41–51.
24. Daffis S, et al. (2010) 2′-O methylation of the viral mRNA cap evades host restriction by IFIT family members. *Nature* 468(7322):452–456.
25. Szretter KJ, et al. (2012) 2′-O methylation of the viral mRNA cap by West Nile virus evades ifit1-dependent and -independent mechanisms of host restriction in vivo. *PLoS Pathog* 8(5):e1002698.
26. Abbas YM, Pichlmair A, Górna MW, Superti-Furga G, Nagar B (2013) Structural basis for viral 5′-PPP-RNA recognition by human IFIT proteins. *Nature* 494(7435):60–64.
27. Sen GC, Fensterl V (2012) Crystal structure of IFIT2 (ISG54) predicts functional properties of IFITs. *Cell Res* 22(10):1407–1409.
28. Sarkar D, Desalle R, Fisher PB (2008) Evolution of MDA-5/RIG-I-dependent innate immunity: Independent evolution by domain grafting. *Proc Natl Acad Sci USA* 105(44): 17040–17045.
29. Ramanathan A, et al. (2015) The autoinhibitory CARD2-Hel2i interface of RIG-I governs RNA selection. *Nucleic Acids* Res, 10.1093/nar/gkv1299.
30. Poeck H, et al. (2008) 5′-Triphosphate-siRNA: Turning gene silencing and Rig-I activation against melanoma. *Nat Med* 14(11):1256–1263.